(Received 21 March 2025, Accepted 9 June 2025, Scheduled 23 June 2025)

Ground Manipulation Techniques for Densified Small Cell Base Stations

Alyaa Syaza Azini* and Tim W. C. Brown

Institute for Communication Systems, University of Surrey, Guildford, Surrey, GU2 7XH, UK

ABSTRACT: Shorter frequency reuse distance in a densified small cell network for fifth generation (5G) could cause more substantial inter-cell interference. Rather than relying on down tilt, it is more necessary to design the azimuth patterns of the antennas to substantially reduce the gain at the sector edges which can reduce the line of sight radiation towards a sector positioned over a reuse distance. The antenna employs a modified ground plane, which utilizes both reflection and diffraction to reduce the gain at the sector edge, and is designed and prototyped from 3.5–4.2 GHz.

1. INTRODUCTION

One of the significant vulnerabilities in small cell densified networks is the co-channel interference among nearby base stations (BSs) with a need for shorter reuse distance. Since the radius of a small cell network is limited with the possibility of a strong line of sight between small cell base stations (SBSs), there is a need to suitably design antennas in a new way to mitigate this problem. A cell sector antenna configuration with suitable azimuth beam patterns is required to minimize the gain at the cell sector edge, which will weaken the line of sight propagation over a given distance. Fig. 1(a) shows a plausible six cell sector cluster topology in a single street canyon with six colors corresponding to six frequency allocations. Note that this is different from the conventional four or seven cell cluster that has been traditionally used for larger cells [1], where the traditionally used coordinate variables i and j are also not applied. Frequency reuse distance is illustrated in Fig. 1 with blue arrows where for example a purple sector may interfere its nearest or vice versa. Clearly where there is a line of sight between the two sectors, a low gain at the sector edge of the left purple sector will help suppress such interference. This sector edge is 60° from the center, and so this provides a desire to reduce gain at $\pm 60°$. The same benefit will be true for the yellow, green, and blue cells. For the red and orange cells on the other hand, it can be assumed that such sectors will benefit from down tilt. Alternatively, an eight sector cluster could be applied so the red and orange cells only have extended reuse distance with brown and turquoise cells shown in Fig. 1(b). Such new paradigms for cell sector clusters to better manage reuse distance will improve capacity in deployments like a heterogeneous fifth generation (5G) small cell network.

Similar to the legacy fourth generation (4G) network, it is assumed that the SBSs consist of up to eight element antenna arrays per BS sector that are vertically orientated with four dual polarized horizontally spaced antenna element pairs stacked vertically. In the literature, base station antenna elements typically consist of a flat reflector [2–4]. Such designs result in high gains at $\pm 60°$ (G_{60}) above -10 dBi in azimuth and wide beamwidth (BW) from the boresight. In this paper, a modified ground plane antenna solution with low G_{60} is introduced. It utilizes integrated reflection and diffraction from the ground plane to manipulate the array pattern not only to reduce G_{60} but also to form a more uniform gain within the cell sector. The final design operating in the 5G pioneer band from 3.4 to 4.2 GHz is validated by measurement. Examples in the literature of horizontal element pairs [5–7] exhibit high G_{60} from each element, typically just 10 dB lower than the boresight gain. Such gain is typically owing to the flat ground plane, and for such arrays in these examples where two elements are spaced horizontally, they will cause vulnerability to interference over the reuse distance when a given beam pattern is formed by precoder phase weights in the array. In this work, the elements are designed with a modified ground plane to have a lower G_{60}, but added features using reflection and diffraction prevent a two element horizontal array from radiating a high G_{60} such that it is more than 10 dB less than what would be radiated with a flat ground plane.

2. ANTENNA ELEMENT RE-SCALING AND GROUND MANIPULATION

Figure 2 shows the antenna radiator adapted and re-tuned from 3.4 to 4.2 GHz [8], which consists of crossed dipoles printed on the bottom of an FR4 substrate of 0.8 mm thickness with a dielectric constant of $\varepsilon_r = 4.55$ and loss tangent of 0.02. The radiator of the antenna with a total dimension of 26×26 mm consists of two pairs of crossed-loop dipoles, and each pair of loop dipoles include outer and inner loops. The inner loop is embedded into the outer loop to generate a new resonant mode to further widen the impedance bandwidth [9]. Each set of dipoles is

* Corresponding author: Alyaa Syaza Azini (alyaa.azini@gmail.com).

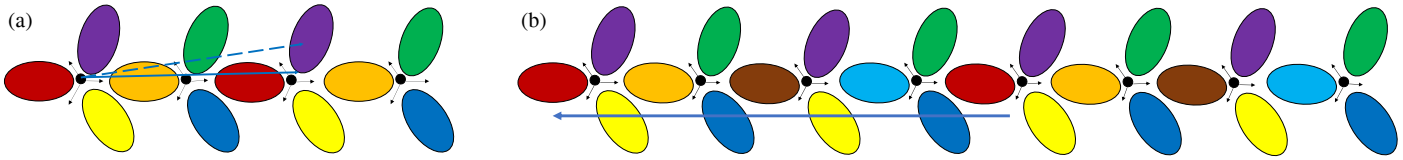

FIGURE 1. Different cell clusters down a single street canyon with (a) six sector reuse distance and (b) extended eight sector reuse distance.

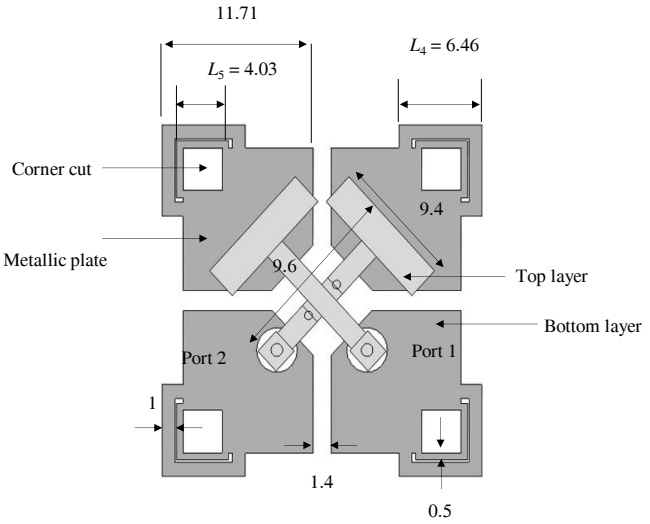

FIGURE 2. Geometry of the antenna radiator (Unit: mm).

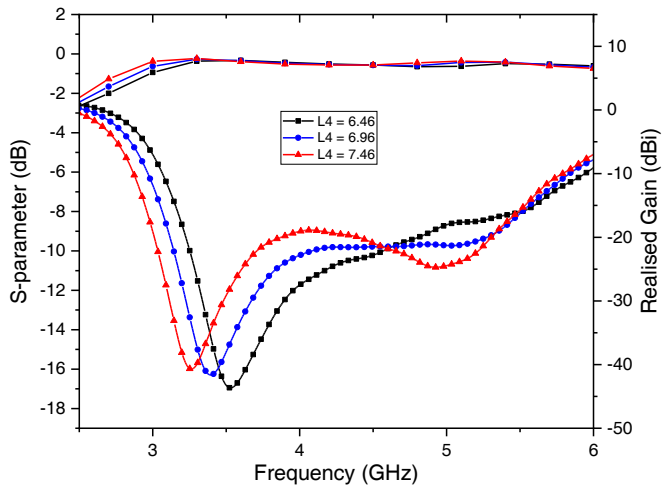

FIGURE 3. Effects of L_4 on $|S_{11}|$ and realized gain for the upper-band antenna.

fed with two T-shaped feeding structures that are printed on the top side of the substrates. One of the feeding structures of the dipoles is altered with a partial feeding line printed on the bottom of the substrates to avoid intersection. The upper part of the feeding structure is connected to the bottom part through two shorting pins. The antenna is fed with a coax feed of 19.8 mm and uses a flat ground plane of total dimension of 150×150 mm. The two loop sizes, L_1 and L_2, were adjusted to cover the frequency range 3.5 to 4.2 GHz. Fig. 3 shows the effects of L_4 on $|S_{11}|$ and realized gain of the upper-band antenna. It can be observed that the upper-band antenna has a stable gain and

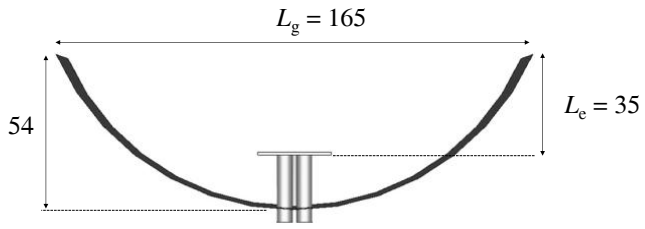

FIGURE 4. Geometry of the circular ground (Unit: mm).

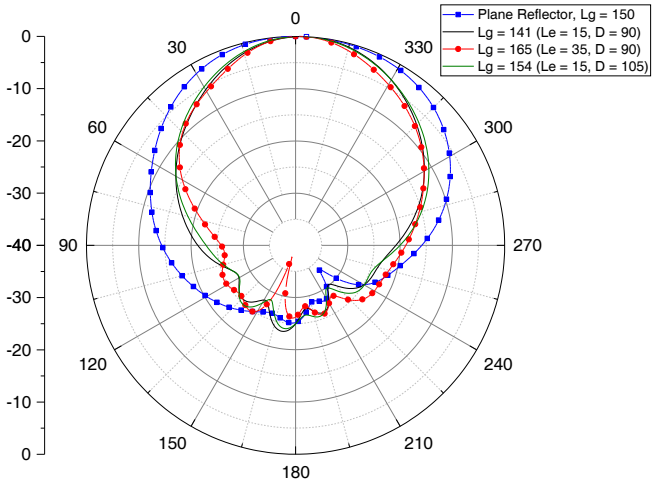

FIGURE 5. Radiation pattern at H-plane at 3.8 GHz for Port 1.

wide impedance bandwidth across its desired band. As shown, the optimum $L_4 = 6.46$ mm is selected in supporting 3.4 to 4.2 GHz.

An appropriate modification to the flat ground is to use a circular reflector ground as in Fig. 4 in order to suitably narrow the beamwidth. The diameter varies from $D = 90$ to 105 mm. For each D, the extended height L_e varies from 15 to 35 mm in height from the antenna's substrate, which results in different values of ground width, L_g. Fig. 5 shows the simulated normalized H-plane ($\phi = 0$) linearly polarized radiation pattern at 3.8 GHz for Port 1. Since the structure of the antenna is highly symmetrical, similar radiation patterns can be obtained when the antenna is excited by port 2. The optimized parameters are $L_g = 165$ mm, $L_e = 35$ mm, and $D = 90$ mm as indicated by the red lines in Fig. 3. Fig. 5 further shows the reduced G_{60} compared to a flat plane reflector.

3. DUAL ANTENNA PLACEMENT

This section extends to a two element dual polarized pair. Their separation is 60 mm or 0.76λ at 3.8 GHz as shown in Fig. 6 to

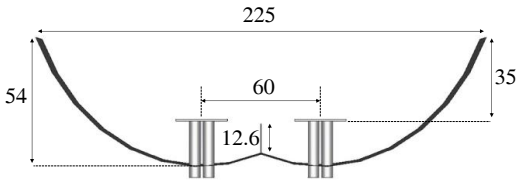

FIGURE 6. Geometry and side view of the circular array antenna (Unit: mm).

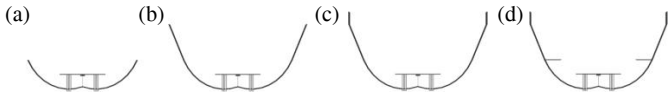

FIGURE 7. An evolution of the stages of the design process. (a) REF 1. (b) REF 2. (c) REF 3. (d) Proposed.

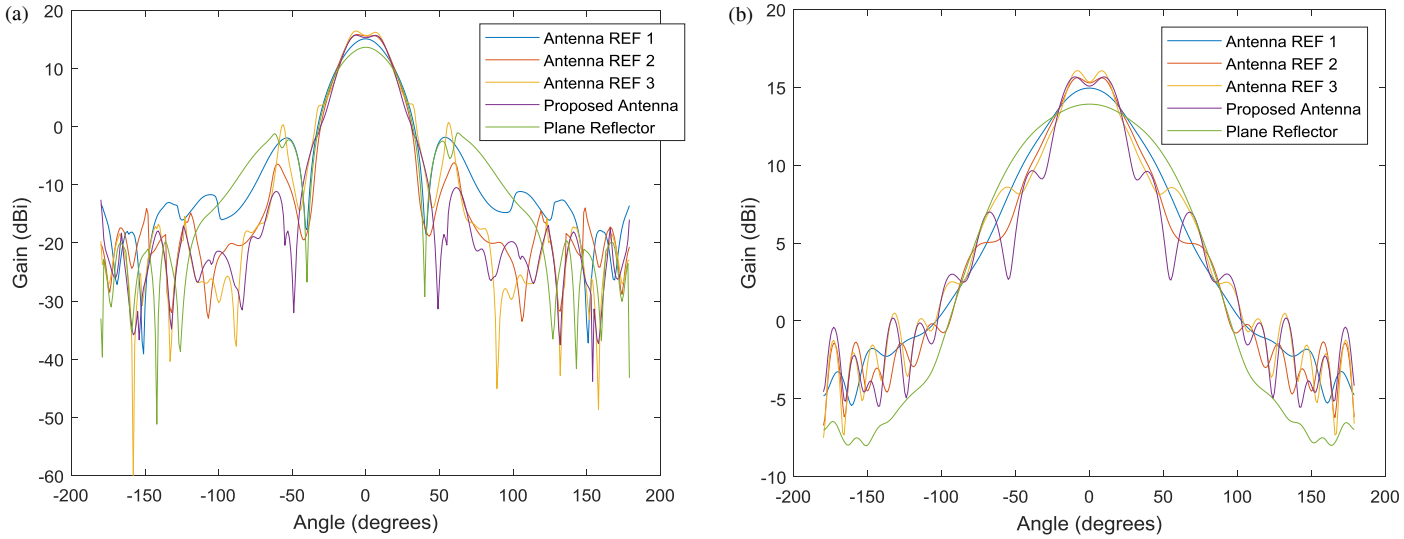

FIGURE 8. Radiation pattern at 3.8 GHz of the design through the evolutionary stages with (a) elements fed with zero phase; (b) array pattern gain envelope.

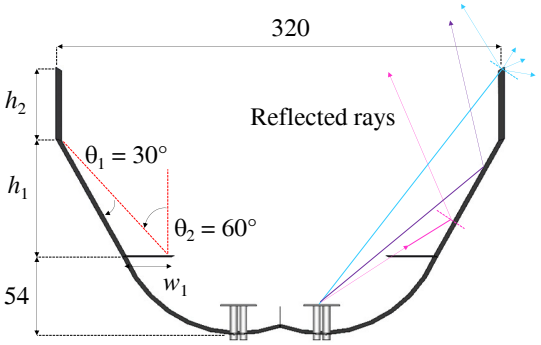

FIGURE 9. Geometry of the final design.

maintain a sufficient portion of the reflector for each element. Such separation will create grating lobes though this is deliberate in this work in order that the combined patterns together with the reflection and diffraction will form the desired pattern structure to provide a wide beam within the cell sector but lower the value of G_{60}. The evolution steps in Fig. 7 show that that from REF 1 to 2 some straight reflectors are introduced while diffractors are introduced in REF 3 and the final step. The effect on the antenna pattern is shown in the array pattern at 3.8 GHz with elements combined with no phase shift in Fig. 8(a), though the two ports of each element are combined with phase inversion to obtain maximum boresight gain. Fig. 8(b), on the other hand, shows the array pattern gain envelope whereby the two elements are co-phased at each angle to ascertain the maximum possible gain in that direction. This finds the worst case scenario when multiple input multiple output (MIMO) pre-coding [10, 11] is applied, and a limit is placed on G_{60}. Clearly, the evolution to the proposed design leads to a solution where G_{60} is suppressed at least 6 dB and as much as 20 dB while within the sector at $\pm 30°$ the beam is widened. This is because the element patterns have been deliberately caused to squint within that region by virtue of using an asymmetric reflector.

Required dimensions for the final proposed design are shown in Fig. 9 consisting of diffraction blockers with width $w_1 = 35$ mm, edge reflectors of height $h_2 = 50$ mm, and side reflectors of height $h_1 = 82$ mm. The diffraction blocker and side reflector are set to form angles θ_1 and θ_2 such that by Snell's laws of reflection fields radiated by the two elements more than $59°$ from the boresight will be caused to undergo diffraction loss and reflect at an angle no less than $-60°$ from the boresight and mirrored vice versa. The absence of the edge reflectors would cause substantial diffraction to spill over the edge of the side reflectors around $\pm 60°$, so the diffraction blockers and side reflectors have optimized dimensions and positions to work together to reduce this. Furthermore, it will allow fields radiated less than $59°$ from the boresight to also reflect more than $-59°$ from the boresight and mirrored vice versa. A slit between the array is inserted because it helps to improve the squint effect with improvement in gain at boresight. The array pattern as well as the array gain pattern envelope is plotted for all frequencies from 3.4 to 4.2 GHz in Figs. 10 (a) and (b) re-

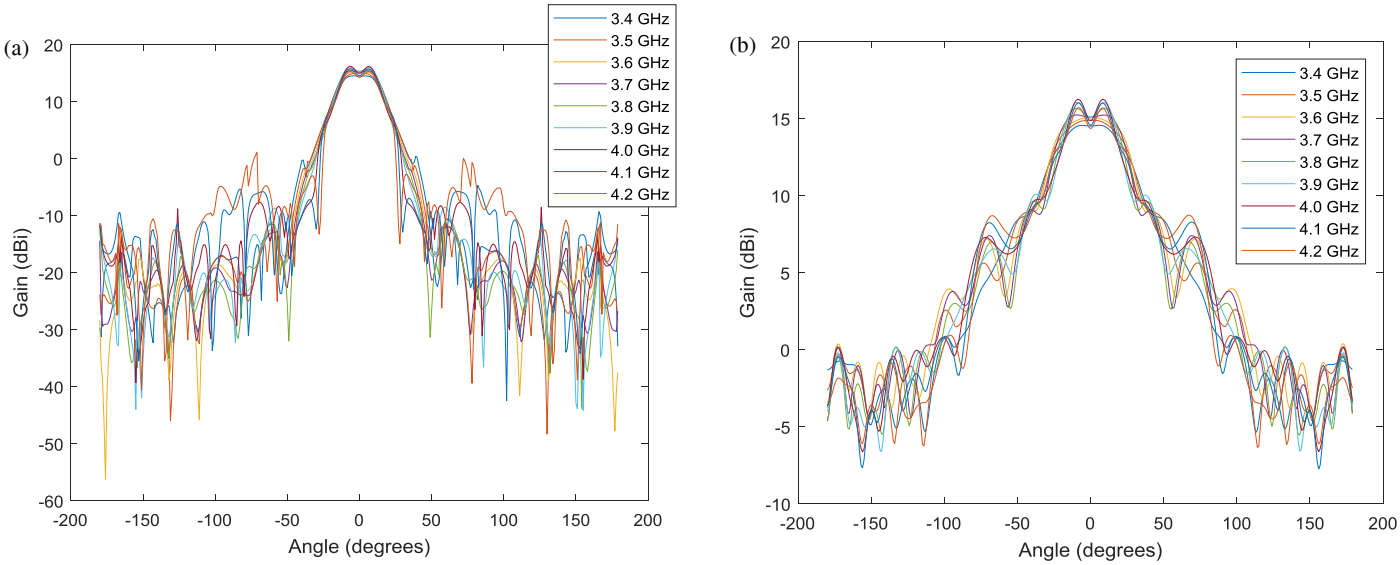

FIGURE 10. Total radiation pattern at each operating frequency when the array antennas received; (a) elements fed with zero phase; (b) array gain pattern envelope.

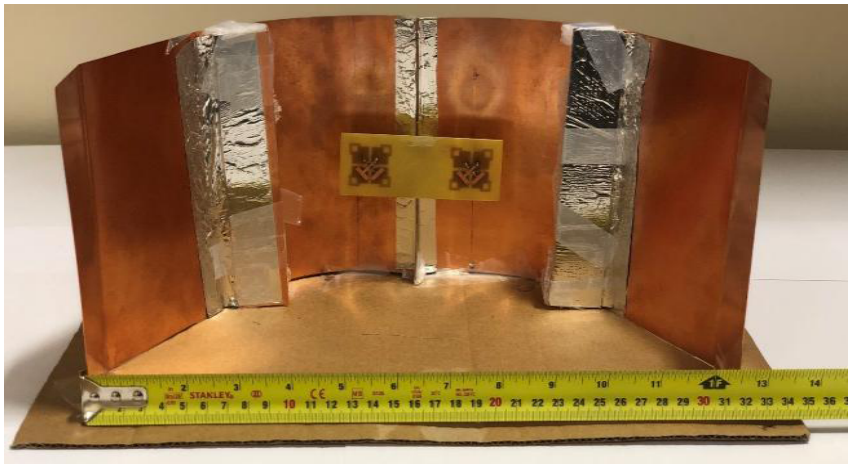

FIGURE 11. Prototype of the antenna array.

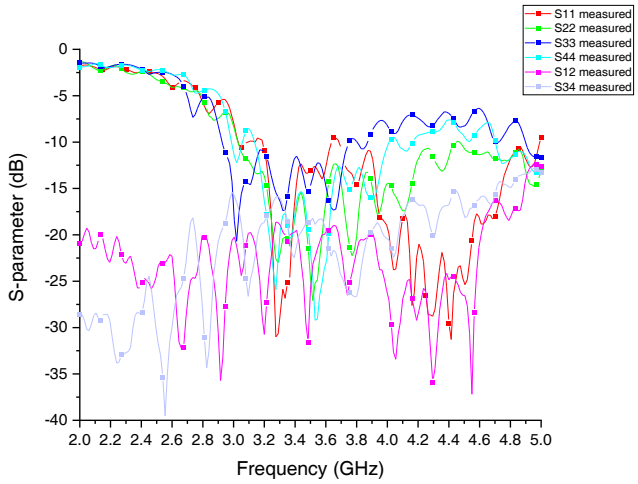

FIGURE 12. Simulated and measured S-parameters of the antenna array.

spectively. Sufficient pattern consistency is shown up to 4 GHz with a modest increase in G_{60} of 6 dB from 4 to 4.2 GHz.

4. MEASUREMENT AND VALIDATION

The antenna array prototype and its measured S-parameters are shown in Figs. 11 and 12, respectively. The measured reflection coefficients S_{11} to S_{44} are less than -10 dB from 3.4 GHz and 4.2 GHz while the highest levels of coupling S_{12} and S_{34} are less than -15 dB. Measured vertical polarizations (V-pol, G_ϕ) are included, as shown in Fig. 13. No significant cross-polarization was found, and the results are not of interest. Three frequencies are chosen where patterns are plotted for all four individual ports at 3.4 GHz, 3.8 GHz, and 4.2 GHz. The gain from each element is shown to fluctuate beyond $\pm 50^\circ$, whereby in general their gain is over 15 dB less than the gain of the main lobe. It is acknowledged that due to defects in structure that some stray lobes appear though they are still further than 10 dB

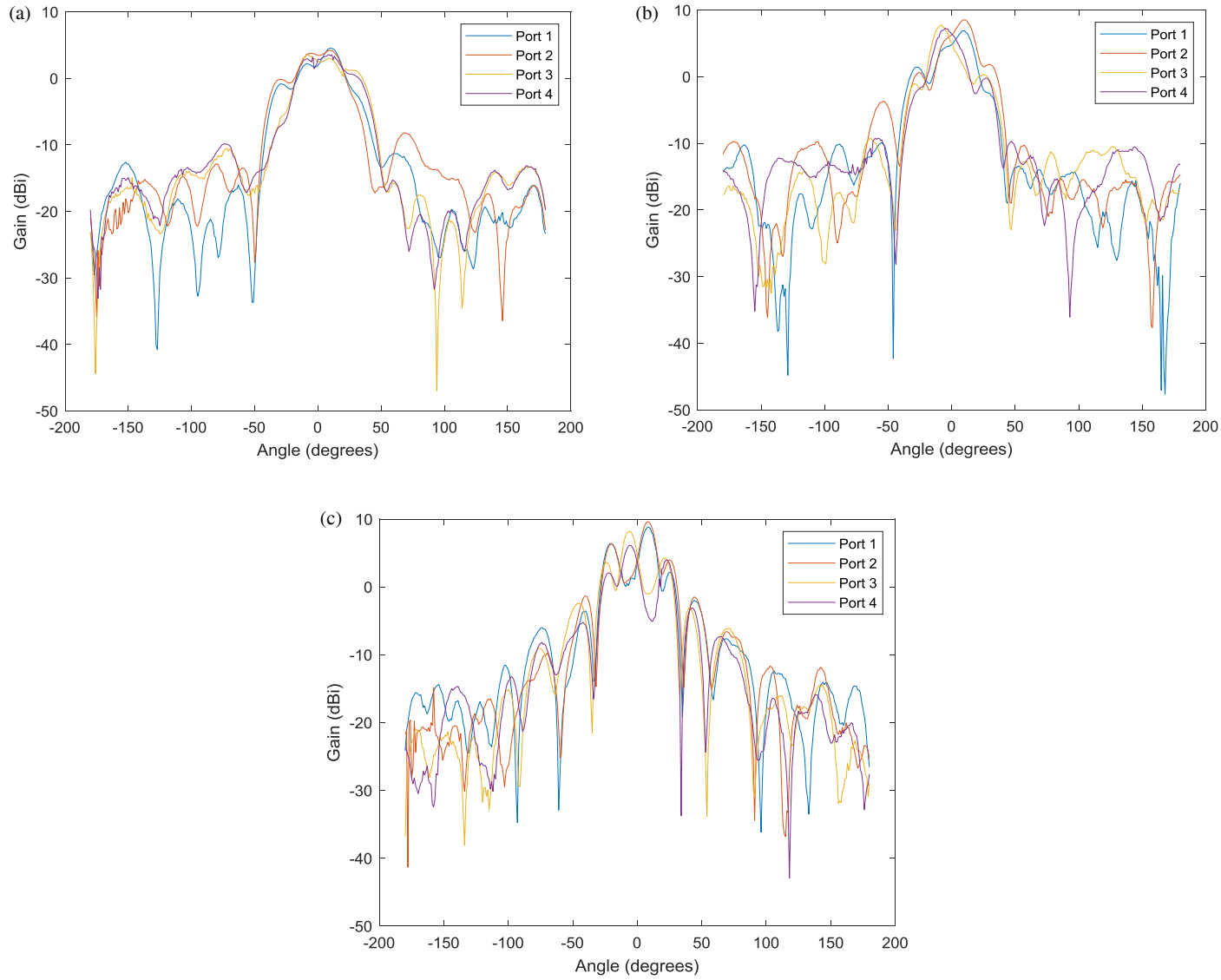

FIGURE 13. Measured radiation patterns of individual ports at (a) 3.4 GHz; (b) 3.8 GHz; and (c) 4.2 GHz.

down from the main lobe to ensure sufficient suppression at the sector edges.

5. CONCLUSION

A new paradigm to design antennas with a low gain at $\pm 60°$ in azimuth to reduce the required reuse distance in densified small base stations below 6 GHz has been presented. A candidate dual polarized two element pair base station antenna prototype for the 5G pioneer bands with an integrated antenna has been designed using integrated diffraction and reflection from a modified ground plane. Four element pairs could be stacked vertically to form an SBS sector antenna through which the line of sight would be suppressed at the sector edge within a cell topology that could be used down a long street canyon. This will help protect against unwanted co-channel interference where the reuse distance is vulnerable to occurring over a line of sight.

REFERENCES

[1] Huang, H., M. Trivellato, A. Hottinen, M. Shafi, P. J. Smith, and R. Valenzuela, "Increasing downlink cellular throughput with limited network MIMO coordination," *IEEE Transactions on Wireless Communications*, Vol. 8, No. 6, 2983–2989, Jun. 2009.

[2] Liu, Y., S. Wang, N. Li, J.-B. Wang, and J. Zhao, "A compact dual-band dual-polarized antenna with filtering structures for sub-6 GHz base station applications," *IEEE Antennas and Wireless Propagation Letters*, Vol. 17, No. 10, 1764–1768, 2018.

[3] Alieldin, A., Y. Huang, S. J. Boyes, M. Stanley, S. D. Joseph, Q. Hua, and D. Lei, "A triple-band dual-polarized indoor base station antenna for 2G, 3G, 4G and sub-6 GHz 5G applications," *IEEE Access*, Vol. 6, 49 209–49 216, 2018.

[4] Feng, B., L. Li, Q. Zeng, and C.-Y.-D. Sim, "A low-profile metamaterial loaded antenna array with anti-interference and polarization reconfigurable characteristics," *IEEE Access*, Vol. 6, 35 578–35 589, 2018.

[5] Chen, Y., J. Zhao, and S. Yang, "A novel stacked antenna configuration and its applications in dual-band shared-aperture base station antenna array designs," *IEEE Transactions on Antennas*

and Propagation, Vol. 67, No. 12, 7234–7241, 2019.

[6] He, D., Q. Yu, Y. Chen, and S. Yang, "Dual-band shared-aperture base station antenna array with electromagnetic transparent antenna elements," *IEEE Transactions on Antennas and Propagation*, Vol. 69, No. 9, 5596–5606, Sep. 2021.

[7] Li, Y. and Q.-X. Chu, "Coplanar dual-band base station antenna array using concept of cavity-backed antennas," *IEEE Transactions on Antennas and Propagation*, Vol. 69, No. 11, 7343–7354, Nov. 2021.

[8] Zheng, D.-Z. and Q.-X. Chu, "A multimode wideband $\pm 45^{\circ}$ dual-polarized antenna with embedded loops," *IEEE Antennas and Wireless Propagation Letters*, Vol. 16, 633–636, 2016.

[9] Chu, Q.-X., D.-L. Wen, and Y. Luo, "Principle of multimode broadband antennas with resonator-loaded dipole," in *2015 International Workshop on Antenna Technology (iWAT)*, 45–47, 2015.

[10] Zhang, Q., H. H. Yang, T. Q. S. Quek, and J. Lee, "Heterogeneous cellular networks with LoS and NLoS transmissions — The role of massive MIMO and small cells," *IEEE Transactions on Wireless Communications*, Vol. 16, No. 12, 7996–8010, Dec. 2017.

[11] Jungnickel, V., K. Manolakis, W. Zirwas, B. Panzner, V. Braun, M. Lossow, M. Sternad, R. Apelfröjd, and T. Svensson, "The role of small cells, coordinated multipoint, and massive MIMO in 5G," *IEEE Communications Magazine*, Vol. 52, No. 5, 44–51, May 2014.